# SUPPLEMENTARY MATERIALS

## Recognition of U-rich RNA by Hfq from the Gram-positive pathogen *Listeria monocytogenes*

**Alexander R. Kovach, Kirsten E. Hoff, John T. Canty, Jillian Orans and Richard G. Brennan***

**Department of Biochemistry, Duke University, Durham, NC 27110, U.S.A.**

**Supplemental Figure 1. One of two alternate Lm Hfq-uracil recognition modes of a total of twelve and the hydrogen bonding network about the ribosyl 2' hydroxyl group.**

**(A)** In addition to positioning residue Q6 by its interaction with residues Q6 and G5", the side chain of residue N42 flips in one of the twelve subunits such that the Nε nitrogen forms a hydrogen bond with the O4 oxygen of uracil. Hydrogen bonding is indicated by blue dashed lines. This conformation is less favoured due to the close approach of the carbonyl oxygens atoms of G5" and Oε of N42.

**(B)** A view of the RNA binding pocket showing the direct hydrogen bond between residue H59 and the ribosyl 2' hydroxyl group and a water-mediated hydrogen bond connecting the carbonyl oxygen of residue F43 to the imidazole side chain of H59 and the 2' hydroxyl group of the ribose sugar.

**Supplemental Figure 2. Superposition of the U-tracts from a variety of Hfq-RNA complexes.**

**(A)** Overlay of all 12 uridine bases from the Lm Hfq–$U_6$ structure using residue H59 as a reference point. The 3' hydroxyl is colored yellow and the 2' hydroxyl group is colored red.

Overlay of the $U_6$ RNA from the Lm Hfq-$U_6$ complex structure (light green) on the proximal-face bound RNAs from **(B)** Sa Hfq-($AU_5G$) complex, (white carbon atoms), **(C)** St Hfq bound to $U_6$ (blue carbon atoms), and **(D)** Ec Hfq bound to $AU_6A$ with only four uridine bases shown (pink carbon atoms).

**Supplemental Figure 3. Sequence alignment of selected Hfq proteins from Gram-positive and Gram-negative bacteria.**

The top eight sequences are those of Gram-positive bacterial Hfq proteins whilst the bottom seven are Hfq protein sequences from Gram-negative bacteria. Key Lm Hfq-RNA interacting residues are listed and their locations denoted by vertical arrows. Adapted from Horstmann *et al.*, 2012.

**Supplemental Figure 4. Lm Hfq-RNA binding isotherms.**

**(A)** Representative binding isotherm of Lm Hfq and $U_6$ RNA in the absence of magnesium ion using fluorescence polarization. The abscissa is the concentration of hexameric Hfq (**micromolar**) and the ordinate is millipolarization. The measured $K_d$ was 3.4 μM.

**(B)** Representative binding isotherm of Lm Hfq and $U_{16}$ RNA using fluorescence polarization. The abscissa is the concentration of hexameric Hfq (**nanomolar**) and the ordinate is millipolarization. The measured $K_d$ was 10.2 nM.

**(C)** Representative binding isotherm of Lm Hfq and $U_6$ RNA in the presence of 10 mM magnesium using fluorescence polarization. The abscissa is the concentration of hexameric Hfq (**nanomolar**) and the ordinate is millipolarization. The measured $K_d$ was 9.9 nM.

**(D)** Representative binding isotherm of Lm Hfq and $U_{15}$dUp RNA in the presence of magnesium using fluorescence polarization. The abscissa is the concentration of hexameric Hfq (**nanomolar**) and the ordinate is millipolarization. The measured $K_d$ was 2.7 nM.

**Supplemental Figure 5. Representative intrinsic tryptophan fluorescence quenching titration experiment.**

To obtain the initial value of tryptophan fluorescence, 1 μM Hfq mutant F26W in the absence of RNA was excited at 298 nm and the emission scanned from 320-400 nm (red scan). The maximum fluorescence intensity is found at 343 nm. RNA quenching of the tryptophan fluorescence is calculated by measuring the intensity differences at wavelength 343 nm after addition of an RNA aliquot, employing the equation Quenching (%) = $(1 - ((F_R-F_B) \div (F_0-F_B))) \times 100$, and carrying out the appropriate corrections as described in the Materials and Methods. The scans after the addition to 1, 2, 3 and 4 μM $A_{15}$ to mutant F26W, which comprises part of the distal-face binding adenine pocket, are colored orange, green, blue and violet, respectively.

**Supplemental Figure 6. The location of Lm HFQ mutants and structure of the proximal face uracil-binding pocket of Lm Hfq (F43W).**

**(A)** View of the proximal face of the Lm Hfq hexamer. Residues mutated for use in tryptophan fluorescence quenching experiments are shown as sticks and colored. Residue F43 is blue and residue R17 is yellow. The remainder of the protein is shown as a grey cartoon and surface.

**(B)** View of the distal face of the Lm Hfq hexamer. Residues mutated for use in tryptophan fluorescence quenching experiments are shown as sticks and colored. Residue F26 is colored red and L33 is green. The remainder of the protein is shown as a grey cartoon and surface.

**(C)** Overlay of Lm Hfq (F43W) and Lm Hfq–$U_6$ RNA complex structures (RMSD = 0.65 **Å)**. The introduced phenylalanine-to-tryptophan mutation does not alter the preformed uracil binding pocket or cause any obvious steric clash with the uridine nucleotide the likely result of which is the same binding affinity of $U_{16}$ fpr F43W and wild type Hfq. The F34W structure is shown as sticks with green carbon atoms and the wild type Hfq is shown as sticks with violet carbon atoms. The RNA from the Lm Hfq-U6 complex structure is shown as sticks and the carbon atoms are colored white.

**(D)** Tryptophan Fluorescence Quenching data using a "negative" control mutant (L33W) on the distal face binding site of Lm Hfq. As expected this residue is not significantly involved in RNA binding and hence is not quenched beyond 10% by any RNA used in this study with the possible exception of $A_{15}$, which is consistent with the known binding mode of $A_{15}$ to the Hfq distal face. Beyond 10% quenching is considered to signify an interaction between Lm Hfq and the tested RNA.

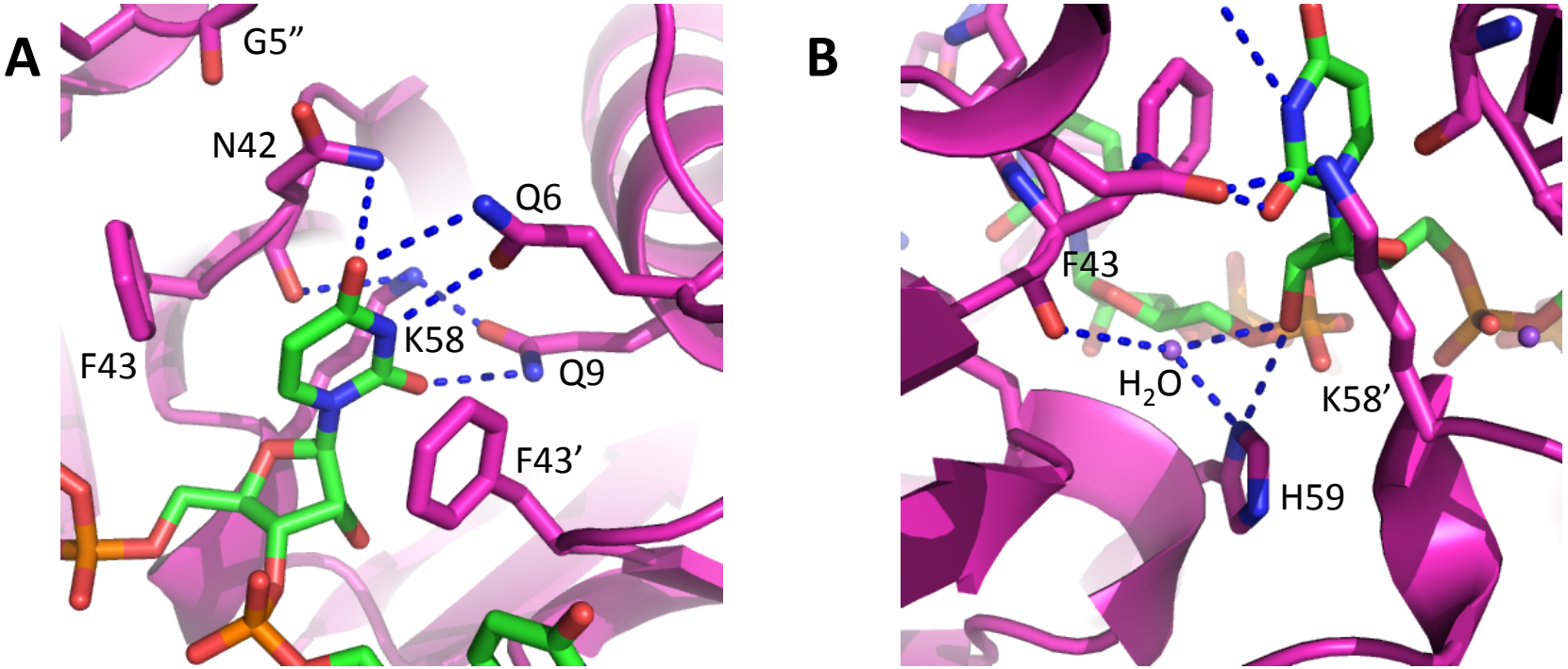


**Supplemental Figure 1**

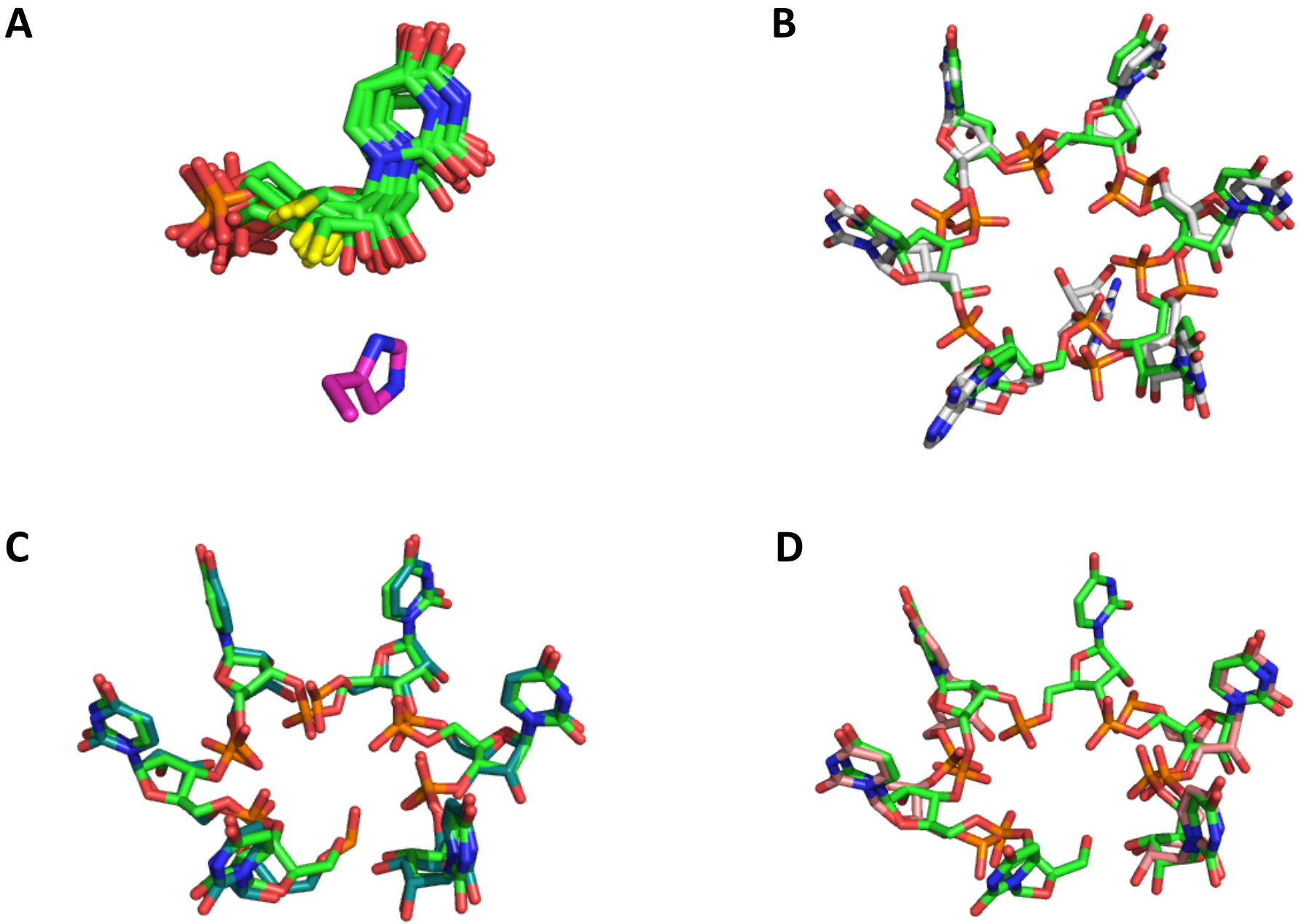


**Supplemental Figure 2**

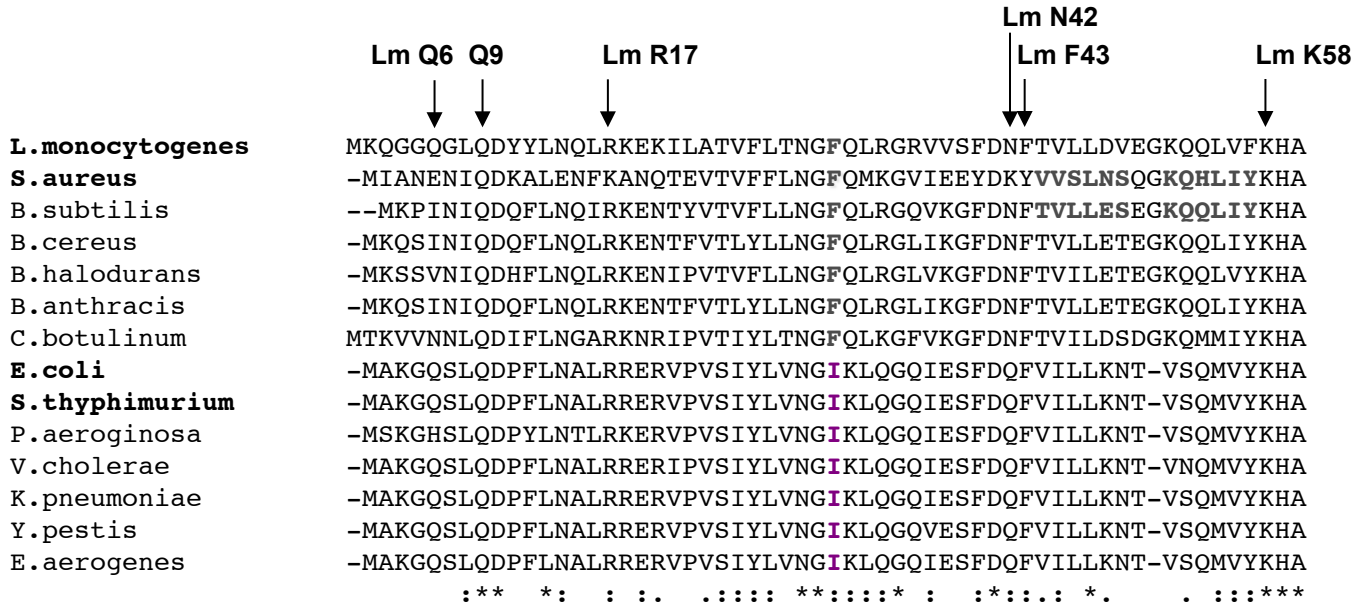


**Supplemental Figure 3**

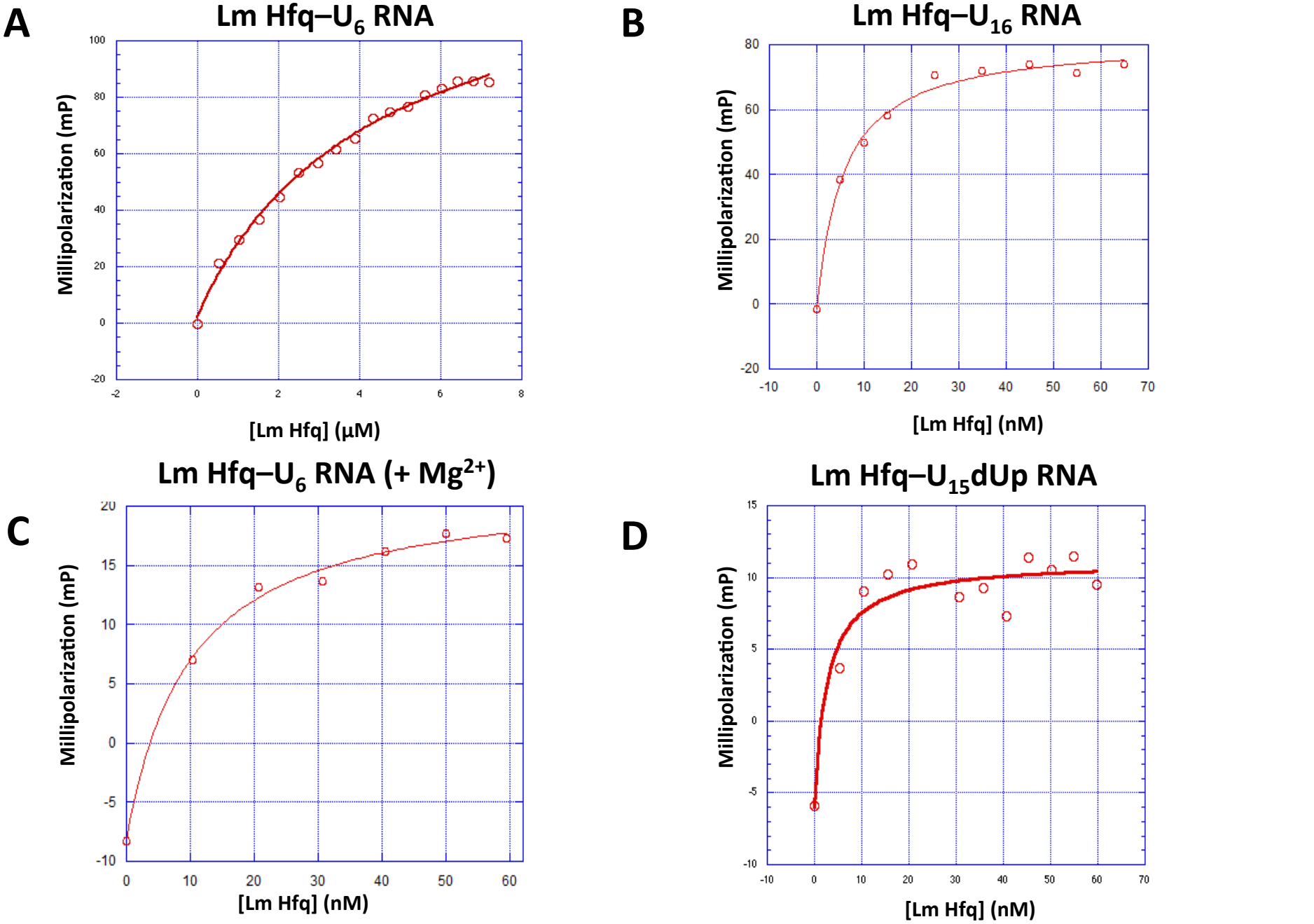


**Supplemental Figure 4**

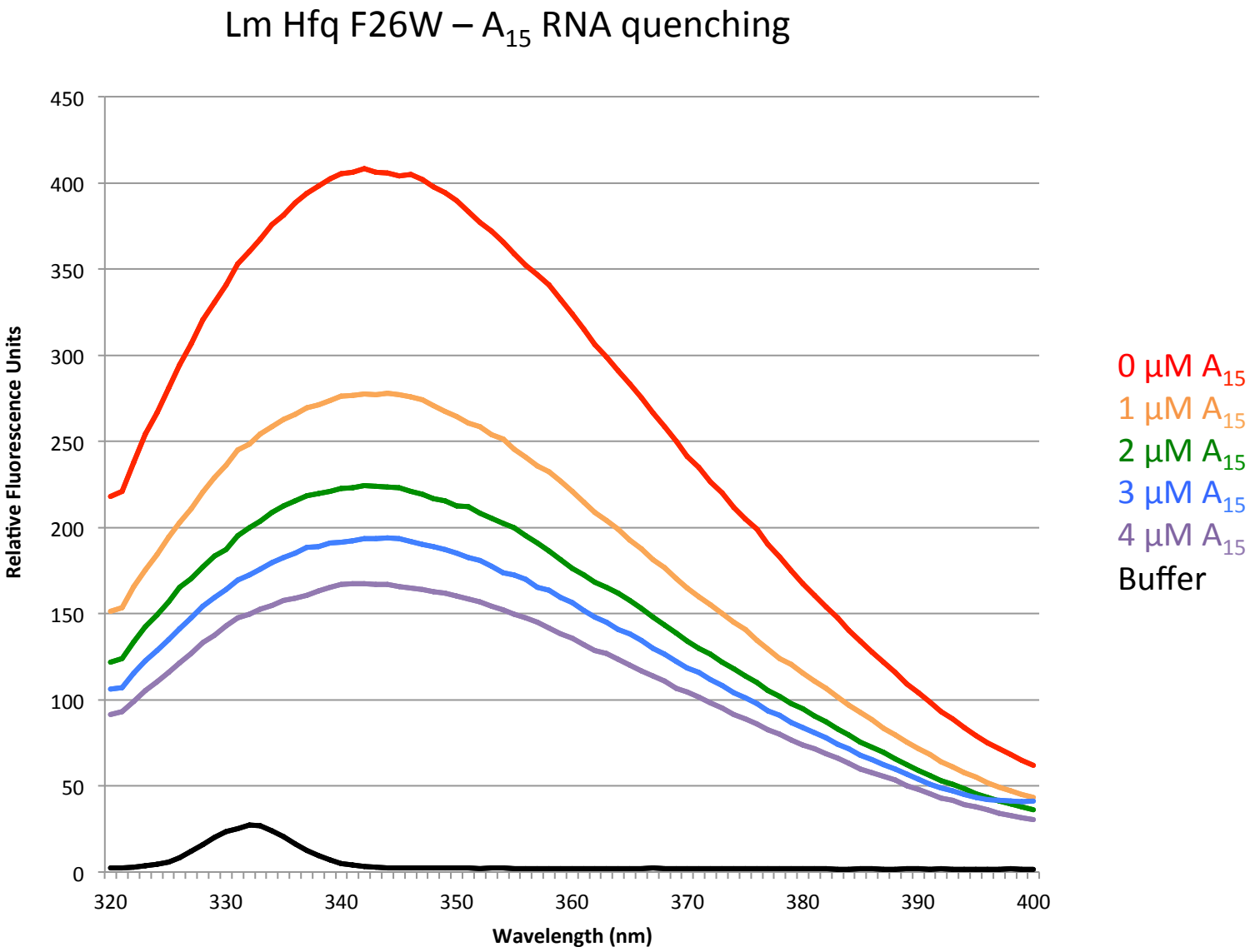


% Quenching = $(1 - ((F_R - F_B) \div (F_0 - F_B))) \times 100$

**Supplemental Figure 5**

A

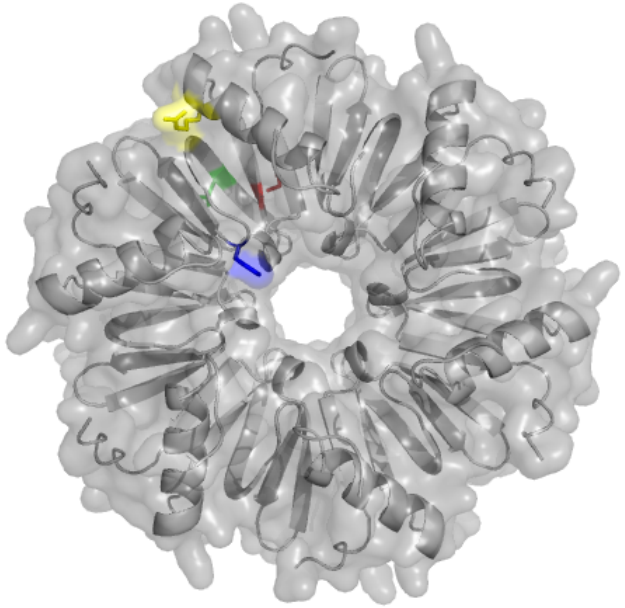

B

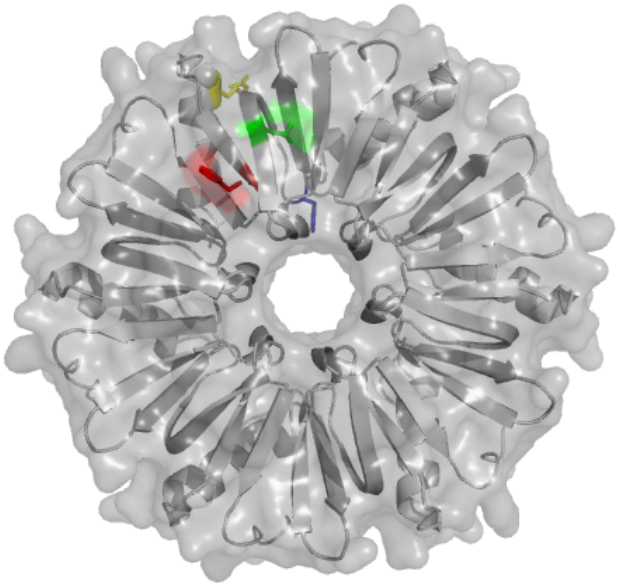

C

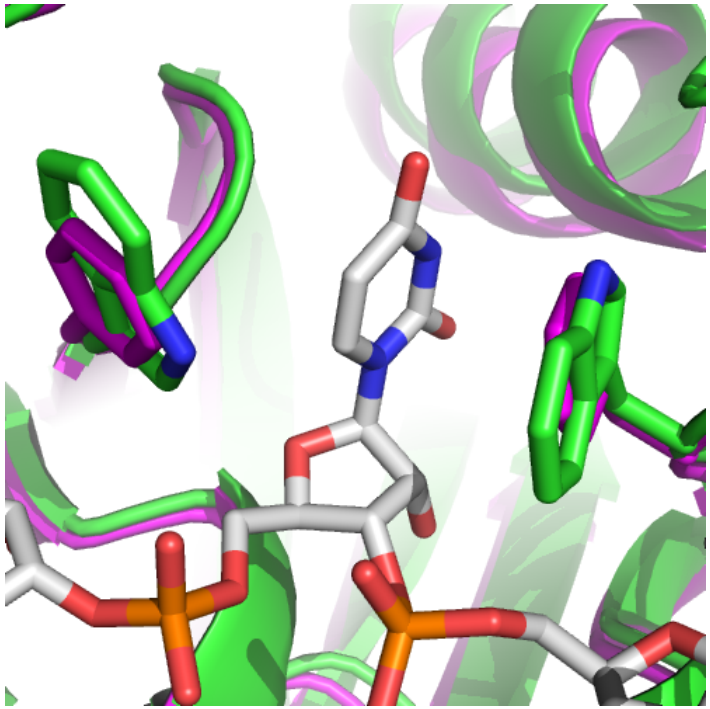

D

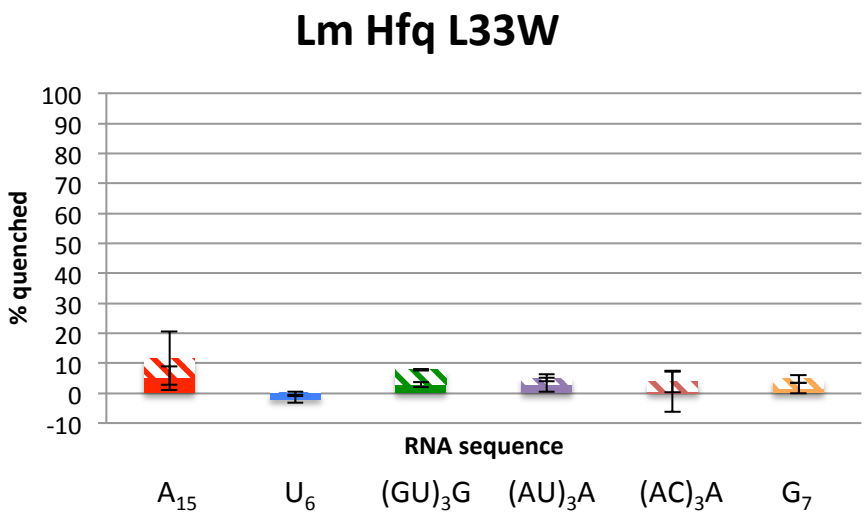


**Supplemental Figure 6**